

## The Effect of Dynamic Focusing of the Beam on the Acoustic Field Distribution Inside the Ultrasonic Ring Array

Wiktor STASZEWSKI\*

*Wrocław University of Science and Technology, Wybrzeże Wyspiańskiego 27,  
50-370 Wrocław, wiktor.staszewski@pwr.edu.pl*

*\*T. Marciniak Lower Silesian Specialist Hospital – Emergency Medicine Centre,  
Gen. Augusta Emila Fieldorfa 2, 54-049 Wrocław*

Tadeusz GUDRA

*Wrocław University of Science and Technology, Wybrzeże Wyspiańskiego 27,  
50-370 Wrocław, tadeusz.gudra@pwr.edu.pl*

### Abstract

This paper presents the analysis of readings acquired from the ultrasonic ring array used in tomography for the diagnosis of female breast tissue. In addition, this paper also presents the results for the acoustic field distribution simulation, acquired through a method of summing up all acoustic fields generated by each of the elementary transducers of the ring array. The change in acoustic field pressure level when changing activation frequency (2 MHz, 3MHz, 4MHz) of the elementary ultrasonic transducers for the sector consisting of 32 and 64 ultrasonic transducers was studied. By changing the time of activation of individual transducers, a change in the natural position of the focus inside the ultrasonic ring array was observed. For the sector consisting of 32 ultrasonic transducers the relation between the echo coming from the wires of the wire pattern and the level of noise and distortion on the ultrasonographic image for different locations of the focus of the central transducers was studied. The results were compared with the simulations of the acoustic field, which were conducted using MATLAB software. This research is the continuation of studies [13, 14] aimed at choosing the optimal focus and number of transducers in ultrasonic ring array with the goal of receiving the best possible quality of images of cross-sections of the female breast.

**Keywords:** ultrasonic ring array, acoustic field distribution, dynamic focusing of ultrasonic beam

### 1. Introduction

Ultrasonic tomography makes early diagnosis of pathological changes in biological tissues possible. There are currently a couple of research centres across the world that analyse the construction and results of ultrasonic tomograph prototypes [1 - 8]. Researchers from the Wrocław University of Science and Technology [6, 7, 9 - 14] are conducting research connected to the use of the ultrasonic transmission tomograph to diagnose female breast tissue. With the aim of receiving the best possible image of the cross-section of the female breast, the acoustic field generated by each of the elementary transducers of the array during dynamic focusing of the ultrasonic beam was analysed. The position of the focus inside the ultrasonic ring array was changed by changing the time of activation of the ultrasonic elementary transducers. The simulation presented in this paper attempted to use the ring array, adapted for ultrasonic transmission tomography, for ultrasonographic imaging. This paper analyses the focusing of the ultrasonic beam generated by either 32 or 64 ultrasonic transducers for their different activation frequencies. Moreover,

an analysis of acquired ultrasonographic images when measuring the wire pattern during the activation of only one section of the ultrasonic ring array consisting of 32 elementary transducers has been conducted [11, 13, 14].

## 2. Construction of the ultrasonic ring array

The ultrasonic ring array made of 32 sections. A section consists of 32 ultrasonic elementary transducers, which are adapted to work in water. The transducers can serve two purposes: they can work as transmitters and as receivers. Each ultrasonic elementary transducer measures 0.5 [mm] x 18 [mm] and is 1 [mm] thick [11]. The beam of the ultrasonic ring array is equal to 130 [mm], and the pitch between the transducers measures 0.3 [mm]. During tests the water had a temperature of 25°C.

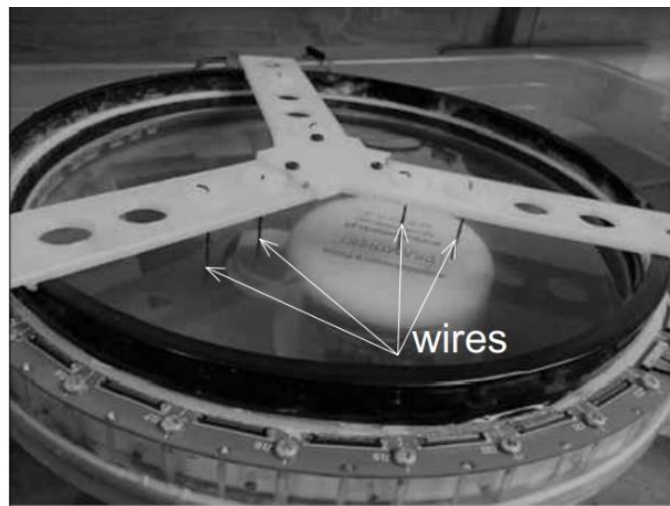


Figure 1. Ultrasonic ring array together with the wire pattern submerged in water that were used in calculations, as viewed from top

## 3. Calculation method

The range of the near field can be calculated based on the following dependency:  $l_o = 0.35a^2/\lambda$ . In the case of resonance frequency  $f_r = 2$  MHz and the width of the ultrasonic elementary transducer  $a = 0.5$  mm the near field range is equal to approximately 12 mm. Beyond this distance a precise analysis of the acoustic field in the central transducer axis in a horizontal plane is possible.

With the goal of determining the acoustic field distribution generated by the curvilinear array of the ultrasonic elementary transducers, a method of calculating the sum of all acoustic fields was applied, as a sum of geometric transformations of fields calculated for all the elementary transducers of the sector (Fig. 2). Simulations for the distribution of acoustic field were conducted using an algorithm obtained according to formula (1).

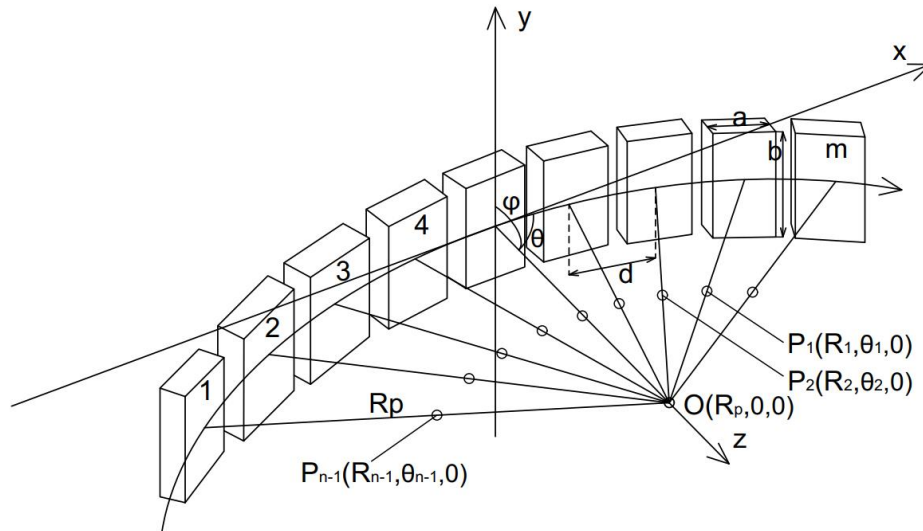


Figure 2. Geometry of the ultrasonic ring array sector showing the sum of acoustic fields of the sector transducers [see also 14]

In this case, the following equation was applied[11, 13, 14]:

$$L_p = 20 \cdot \log \left( \left| \sum_{i=0}^{m-1} -\frac{j\rho ckV_a}{2\pi R_i} ab \cdot e^{j(\omega t - kR_i)} \left( \frac{\sin\left(\frac{u_i a}{2}\right)}{\frac{u_i a}{2}} \right) \left( \frac{\sin\left(\frac{wb}{2}\right)}{\frac{wb}{2}} \right) \right| \cdot \frac{1}{p_o} \right) \quad (1)$$

where:  $\rho$  – density of the medium,  
 $c$  – ultrasonic wave propagation velocity in the medium,  
 $k = 2\pi/\lambda$  – wavenumber,  
 $\lambda = c/f$  – wavelength,  
 $f$  – resonance frequency of the ring array transducers,  
 $\omega = 2\pi f$  – cycle resonance frequency of pulsations,  
 $t$  – time,  
 $V_a$  – acoustic velocity,  
 $p_o$  – reference pressure ( $p_o = 1 \mu\text{Pa}$ ),  
 $a$  – width of the elementary rectangular transducer,  
 $b$  – length of the elementary rectangular transducer,  
 $m$  – number of transducers in the ring array sector,  
 $u_i = 2\pi \cdot \sin(\theta_i)/\lambda$ ,  
 $w = 2\pi \cdot \sin(\varphi)/\lambda$ ,  
 $R_i, \theta_i, \varphi$  – polar coordinates of the point  $P(R, \theta, \varphi)$ , corrected in respect of the location  $(i+1)$ th transducer in sector.

The geometrical transformation of the location of every point of the field  $P(R, \theta, \varphi)$  in equation (1) is carried out symmetrically for every  $i + 1$ th transducer in the ring array sector (Fig. 2) by turning the point around the symmetry axis of the array with coordinates  $O(r = R_p, \theta = 0)$  parallel to the  $Y$  axis (where  $R_p$  denotes the array's internal radius) by an appropriate multiplicity of the angle  $\beta = i \cdot 2\pi/N$  (where  $N$  is the number of all the transducers in the ring array). Revised coordinates for  $P(R, \theta, \varphi)$  for following revolutions in the polar system (occurring in formula (1)) can be determined using formulae [11, 13, 14]:

$$\begin{cases} r_i = \sqrt{r^2 + 4R_p^2 \sin^2 \frac{\beta_i}{2} + 2rR_p \cos(\theta - \beta_i) - 2R_p \cos \theta} \\ \theta_i = \arctg \left( \frac{r \sin(\theta - \beta_i) + R_p \sin(\beta_i)}{r \cos(\theta - \beta_i) + 2R_p \sin^2 \frac{\beta_i}{2}} \right) \end{cases} \quad (2)$$

$$\beta_i = \left( \frac{m-1}{2} - i \right) \cdot \beta \quad (3)$$

where  $i = 0, \dots, m-1$ .

#### 4. Results

When taking the readings with the use of linear phased (steered) scanning, the ultrasonic ring array was submerged in distilled water with a temperature of 25°C. The method of dynamic focusing was applied; by changing the time of activation of the ultrasonic elementary transducers the position of the focus was changed. This caused the focus to move closer or farther apart along the axis between two central transducers and a point where natural focus occurs due to the curvature of the ring array. During readings, the section of the ring array consisting of 32 ultrasonic elementary transducers was used. The readings were taken for nine different distances between the focus and central transducers. Each reading was taken in identical conditions. The wires of the wire pattern had the same thickness and were made of the same material. The results of the readings are presented in (Fig. 3). Next, the acquired ultrasonographic images of the wire pattern were analysed.

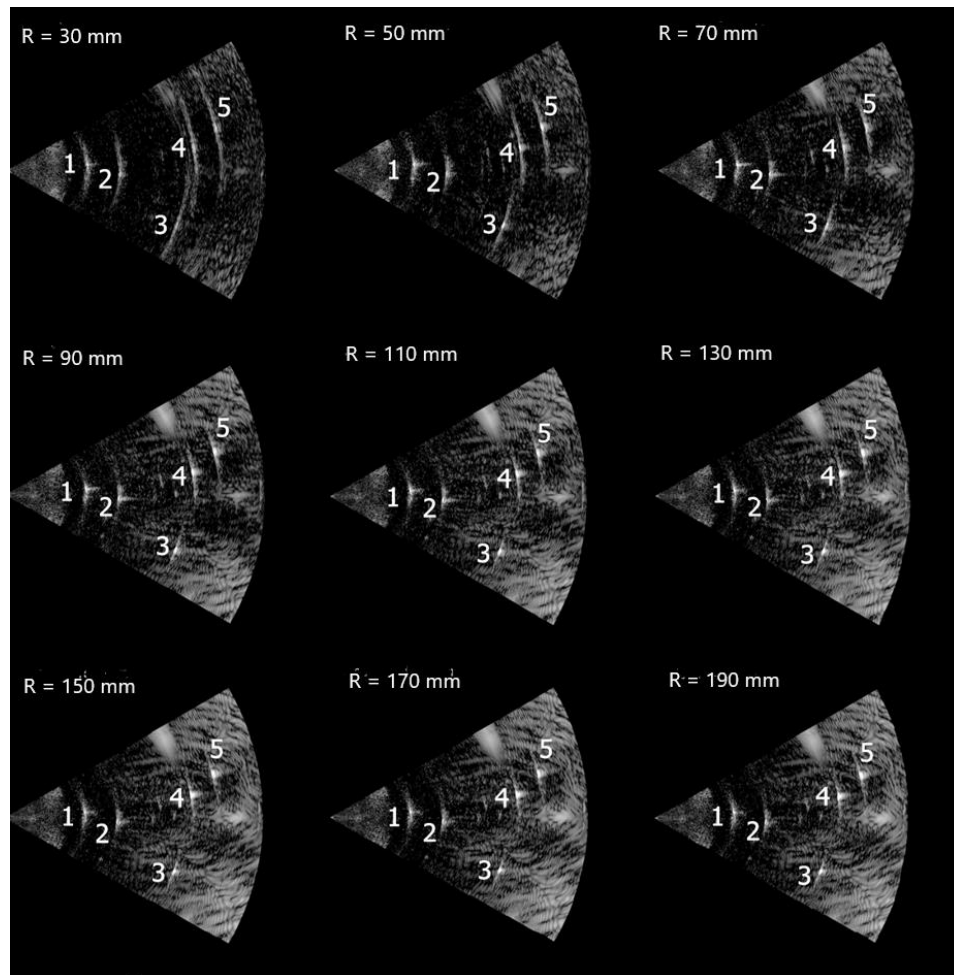


Figure 3. Results of readings of the wire pattern using the ultrasonic ring array with  $n = 32$  activated ultrasonic transducers with the focus at the following intervals  $R = 30$  mm,  $R = 50$  mm,  $R = 70$  mm,  $R = 90$  mm,  $R = 110$  mm,  $R = 130$  mm,  $R = 150$  mm,  $R = 170$  mm and  $R = 190$  mm with numbered echoes coming from the rods [see also 14]

Table (1) shows the analysed data from the ultrasonographic images (Fig. 3) during dynamic focusing. The relationship between an average level of noise and distortion occurring around the analysed inclusion and the brightness of the inclusion coming from the wires of the pattern was recorded using a greyscale. The results for each of the identified inclusion are presented in percentages in the table below.

Table 1. The relationship between an average level of noise and distortion to the brightness of the inclusion coming from the wire of the wire pattern

| R [mm] | point 1 | point 2 | point 3 | point 4 | point 5 | average |
|--------|---------|---------|---------|---------|---------|---------|
| 30     | 32.74   | 18.95   | 60.44   | 56.76   | 59.96   | 45.77   |
| 50     | 26.46   | 17.10   | 48.16   | 38.52   | 52.79   | 36.61   |
| 70     | 28.69   | 38.96   | 58.47   | 51.59   | 57.37   | 47.01   |
| 90     | 30.45   | 33.21   | 66.70   | 55.87   | 60.46   | 49.34   |
| 110    | 32.91   | 36.81   | 58.36   | 61.53   | 64.08   | 50.74   |
| 130    | 38.61   | 37.74   | 55.87   | 62.84   | 62.99   | 51.61   |
| 150    | 37.78   | 35.91   | 55.82   | 60.91   | 61.18   | 50.32   |
| 170    | 40.28   | 46.92   | 60.08   | 60.08   | 59.61   | 53.40   |
| 190    | 42.63   | 45.72   | 61.11   | 59.60   | 61.18   | 54.05   |

Next, it was analysed how a change in activation frequency of the ultrasonic elementary transducers affected the acoustic pressure in the focus. A simulation of acoustic field pressure for activation frequencies 2 MHz, 3 MHz and 4 MHz was conducted using formula (1) for 32 and 64 activated ultrasonic transducers. Moreover, it was checked how a 10° inclination of the beam affected the acoustic pressure in the focus. The results are presented in graphs 4 and 5.

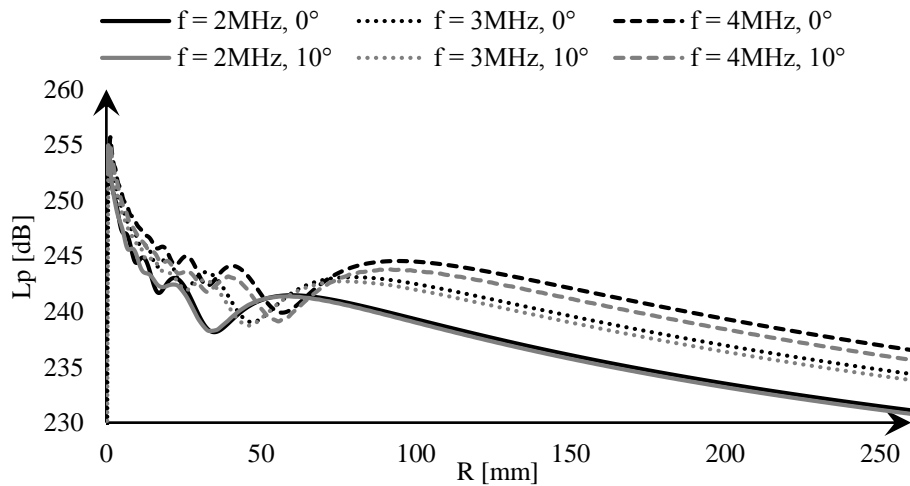


Figure 4. Results of the acoustic field distribution calculations in the form of  $L_p(z)$  with a number of activated transducers  $m = 32$ , for  $f = 2$  MHz, 3 MHz and 4 MHz without and with a 10° inclination of the beam

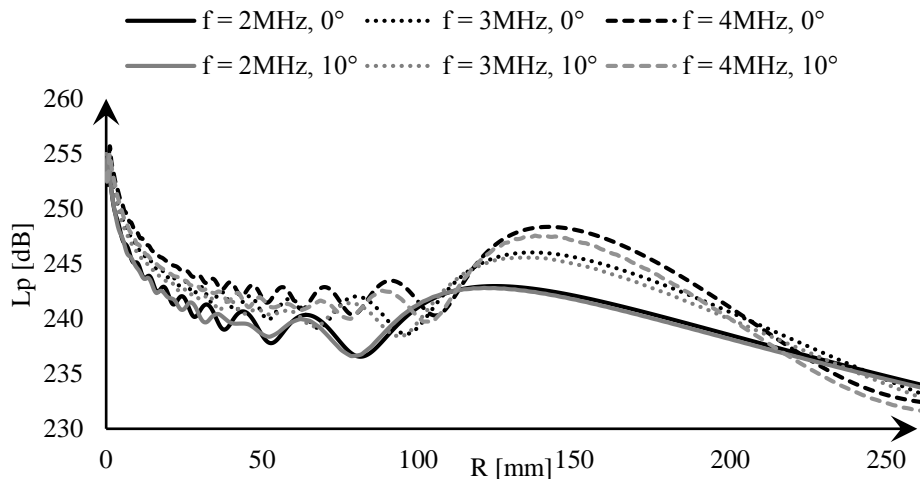


Figure 5. Results of the acoustic field distribution calculations in the form of  $L_p(z)$  with a number of activated transducers  $m = 64$ , for  $f = 2$  MHz, 3 MHz and 4 MHz without and with a  $10^\circ$  inclination of the beam

## 5. Conclusions

After analysing the results of the wire pattern readings, it can be stated that the smallest ratio of noise and distortion level to the echo coming from the inclusion occurs for the focus positioned 50 [mm] away from central transducers, in which average worth of this relationship for all echoes equalled 36.61[ %]. Based on analysis of these readings, it can be concluded that the most beneficial focus for analysing the cross-sections of the female breast occurs 50 [mm] away from central transducers, because the acquired ultrasonographic images had the biggest contrast.

Based on the analysis of sections consisting of 32 and 64 ultrasonic elementary transducers it can be concluded, that the level of acoustic pressure in the focus occurring due to the natural curvature of the ring array increases together with activation frequency of the ultrasonic elementary transducers despite using the same ultrasonic transducers. In the case of a  $10^\circ$  inclination of the beam, the level of acoustic pressure decreased on average by 1 [dB] for three of the analysed frequencies. This means that the beam can be inclined in this range without deterioration of its parameters. That is why, when acquiring an image consisting of 32 sections made up of 32 transducers, a significant reduction in noise and distortion can be achieved by averaging out the pixels.

## References

1. M. Birk, E. Kretzek, P. Figuli et al., *High-speed medical imaging in 3D ultrasound computer tomography*, IEEE Trans. Parallel Distrib. Syst., **27**(2) (2016) 455 – 467.
2. F. A. Duck, *Physical Properties of Tissue - A Comprehensive Reference Book*, Academic Press London 1990.

3. N. Duric, P. Littrup, L. Poulou et al., *Detection of breast cancer with ultrasound tomography: first results with the Computed Ultrasound Risk Evaluation (CURE) prototype*, Med. Phys., **34**(2) (2007) 773 – 785.
4. N. Duric, P. Littrup, S. Schmidt et al., *Breast imaging with the SoftVue imaging system: first results*, In: J. G. Bosch, M. M. Doyley (Eds.), *Medical Imaging: Ultrasonic Imaging, Tomography, and Therapy*, Proc of SPIE.SPIE, p. 8675 (2013) 86750K-1-8.
5. R. Entrekin, P. Jackson, J. R. Jago, B. A. Porter, *Real Time Spatial Compound Imaging in Breast Ultrasound: Technology and Early Clinical Experience*, Medica-Mundi, **43**(3) (1999) 35 – 43.
6. T. Gudra, K. Opieliński, *The ultrasonic probe for investigating of internal object structure by ultrasound transmission tomography*, Ultrasonics, **44** (2006) e679 – e683.
7. T. Gudra, K. Opieliński, *The multi-element probes for ultrasound transmission tomography*, Journal de Physique IV, **137** (2006) 79 – 86.
8. T. Gudra, K. J. Opieliński, *Sposób wizualizacji struktury wewnętrznej ośrodka i urządzenie do realizacji tego sposobu*, Patent, Polska, Nr 210202.
9. R. Jirik, I. Peterlík, N. Ruiter et al., *Sound-speed image reconstruction in sparse-aperture 3-D ultrasound transmission tomography*, IEEE Trans. Ultrason. Ferroelectr. Freq. Control, **59**(2) (2012) 254 – 264.
10. V. Z. Marmarelis, J. Jeong et al., *High-resolution 3-D imaging and tissue differentiation with transmission tomography*, Acoust. Image, **28** (2007) 195 – 206.
11. K. J. Opieliński, *Application of Transmission of Ultrasonic Waves for Characterization and Imaging of Biological Media Structures*, Printing House of Wrocław University of Science and Technology, Wrocław 2011 [in Polish].
12. K. J. Opielinski, P. Pruchnicki, T. Gudra, J. Majewski, *Full angle ultrasound spatial compound imaging*. In: *Proceedings of 7<sup>th</sup> Forum Acusticum 2014 Joined with 61<sup>st</sup> Open Seminar on Acoustics and Polish Acoustical Society –Acoustical Society of Japan Special Session Stream [CD-ROM]*, Krakow: European Acoustics Association (ISSN 2221-3767), 2014.
13. W. Staszewski, T. Gudra, K. J. Opieliński, *The acoustic field distribution inside the ultrasonic ring array*, Archives of Acoustics, **43**(3) (2018) 455 – 463.
14. W. Staszewski, T. Gudra, K. J. Opieliński, *The effect of dynamic beam deflection and focus shift on the acoustic field distribution inside the ultrasonic ring array*, Archives of Acoustics, 2019 (article submitted to the editorial office).